Journal of Structural Geology, Vol. 11, No. 4, pp. 421 to 431, 1989
Printed in Great Britain

0191-8141/89 $03.00 + 0.00

Cover deformation above a blind duplex: an example from West Virginia, U.S.A.

DAVID A. FERRILL* and WILLIAM M. DUNNE†

Department of Geology and Geography, West Virginia University, Morgantown, WV 26506, U.S.A.

(*Received* 6 *October* 1987; *accepted in revised form* 24 *September* 1988)

Abstract—Pretectonic cover above blind thrust systems responds to underlying thrusting by combinations of forethrusting, backthrusting and coupling. The role of these responses was examined in the Hanging Rock–Cacapon Mountain anticlinorium of the central Appalachians. This cover fold consists of Middle Ordovician and younger sedimentary rocks above a blind horse of Cambro-Ordovician carbonates. The cover has abundant folding and subsidiary faulting. Cover cleavage in carbonate and fine-grained clastic rocks formed before regional folding in response to layer-parallel shortening (LPS). This 15% LPS also produced grain-suturing and fluid-inclusion trails in quartzarenites. The LPS formed during cover forethrusting, accommodating older blind horses in the hinterland. With the formation of the underlying horse, cover coupling occurred with bending–folding, additional secondary buckling and cleavage rotation by flexural flow with perhaps minor flattening. This cover coupling was insufficient to accommodate horse formation. No evidence exists for backthrusting, but forelandwards, abundant subsurface evidence exists for cover forethrusting with imbricate thrusting. This thrusting accommodates horse formation and differs in style from the LPS of the older forethrusting event. So, for this blind system, the cover responded with a combination of coupling and forethrusting.

INTRODUCTION

A DISTINCTIVE feature of blind thrust systems is an overlying cover of coevally deforming rocks (Jones 1982, Banks & Warburton 1986, Morley 1986a, Geiser 1988). As shown in Fig. 1, a pre-existing cover responds over blind systems by forethrusting (Geiser 1988), backthrusting (Jones 1982, McMechan 1985, Banks & Warburton 1986), or coupling (Ferrill & Dunne 1986, Dunne & Ferrill 1988).

For forethrusting (Fig. 1a), the cover is pinned to the blind system behind the leading branch line. The cover displaces toward the foreland, forming upright or foreland-verging folds and cleavage, and imbricate forethrusts (Marshak & Engelder 1985, Geiser 1988). For backthrusting (Fig. 1b), the cover is pinned at the leading branch or tip line. The cover displaces toward the hinterland with respect to the underlying thrust, forming hinterland-verging folds and cleavage, and imbricate backthrusts (Suppe 1983, McMechan 1985, Banks & Warburton 1986, Morley 1986a, b). For coupling (Fig. 1c), the cover is also pinned at the leading branch or tip line, but the cover deforms locally without a regionally consistent transport direction, producing upright and locally-verging folds, vertical or axial-planar cleavage, and local forethrusts and backthrusts.

The existence of these cover responses has recently been documented above blind thrust systems in the Canadian Rockies (McMechan 1985), Norway (Morley 1986b), Spain (De Poar & Anastasio 1987), Pakistan (Banks & Warburton 1986) and Taiwan (Suppe 1983). In the blind thrust system of the central Appalachians, recent workers have described cover structures (Perry 1979, Herman 1984, Kulander & Dean 1986, Mitra 1986) and have attributed the deformation to forethrusting (Perry 1978, Herman 1984, Mitra 1986, Geiser 1988).

A primary, and sometimes the only, criterion for proposing forethrusting is that it is necessitated by the piggyback or footwall imbrication of the blind thrust system. However, backthrusting is the dominant cover response in other blind piggyback thrust systems (Suppe 1983, McMechan 1985, Banks & Warburton 1986). Therefore, the purposes of this paper are (1) to compare shortening magnitudes and structural styles between a blind duplex and its overlying cover in the central Appalachians; (2) to partition the cover deformation by

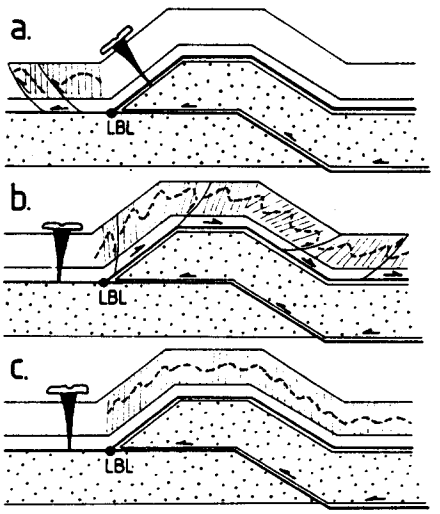

Fig. 1. Cover responses to blind thrusting. (a) Forethrusting, (b) backthrusting and (c) coupling. Dashed lines are schematic cover folds, thin lines show cleavage geometry and LBL is leading branch line.

*Present address: Department of Geology, University of Alabama, Tuscaloosa, AL 35487, U.S.A.
†Present address: Department of Geological Sciences, University of Tennessee, Knoxville, TN 37916, U.S.A.

the type of cover responses; and (3) to present a kinematic model for the progressive deformation of the cover and underlying duplex.

GEOLOGIC SETTING

The Appalachian Valley and Ridge Province in West Virginia (Fig. 2) contains a blind thrust system that formed during the Pennsylvanian–Permian Alleghenian orogeny (Perry 1978, Geiser & Engelder 1983). The thrust system consists of blind duplexes, which deformed Cambro-Ordovician carbonates (Fig. 3, coarse stipple) between a floor thrust in the Lower Cambrian Waynesboro (Rome) Formation and a roof thrust in the Middle Ordovician Martinsburg Formation (Kulander & Dean 1986, Mitra 1986). The cover above the roof thrust consists of Middle Ordovician through Mississippian clastic and carbonate sedimentary rocks. These cover rocks are pretectonic because they are older than the Alleghenian thrusting. Hence, they coevally deformed above the blind duplexes by some combination of forethrusting, backthrusting and coupling.

In the Valley and Ridge Province of West Virginia, recent workers have proposed a major role for faulting in cover deformation. This idea has foundations in the groundbreaking work of Jacobeen & Kanes (1974), which established the existence of imbricate faults in the cover by using seismic reflection data (Figs. 3a & b). However, recent workers differ greatly regarding the geometry of cover imbrication, despite the ubiquitous use of seismic reflection data. In one geometry, the cover contains both isolated and linked forethrusts and backthrusts (Fig. 3c) (Kulander & Dean 1986). In a second geometry, the cover contains a footwall-imbricated duplex overlain by a footwall-imbricated imbricate fan (Fig. 3d) (Mitra 1986). The present study area was investigated to determine which of these proposals, if either, applied to the cover rocks at the surface.

The study area is located in eastern West Virginia along the Hanging Rock–Cacapon Mountain anticlinorium (HRA, Fig. 2). This cover anticlinorium is above an extensive blind duplex that changes geometry along strike (Perry & De Witt 1977, Kulander & Dean 1986, Mitra 1986). In the study area, the main folds in the anticlinorium are the Hanging Rock and Baker Mountain anticlines (Figs. 4 and 3c & d). Rocks cropping out at the surface range from the Upper Ordovician Juniata Formation, through the Siluro-Devonian Helderberg Group, to the Devonian shales (Fig. 4).

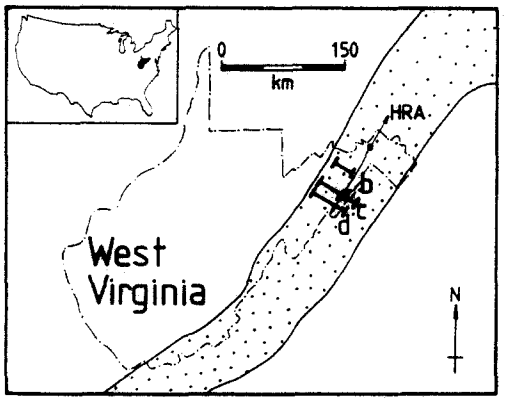

Fig.2 Location of study area (small rhomb shape) in West Virginia. Inset map shows location of West Virginia in the U.S.A. Stipple represents Valley and Ridge Province. HRA is Hanging Rock–Cacapon Mountain anticlinorium. Lines b, c and d locate sections in Figs. 3(b), (c) & (d).

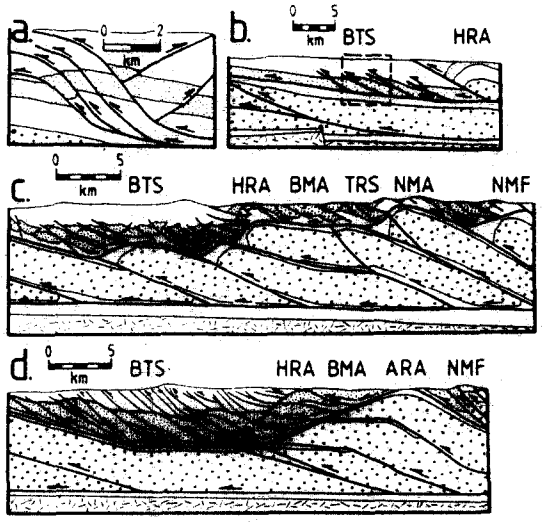

Fig. 3. Cross-sections across central Valley and Ridge Province. (a) and (b) modified from Jacobeen & Kanes (1974) and (a) is inset of (b). (c) modified from Kulander & Dean (1986, section 3). (d) modified from Mitra (1986, fig. 10). (Abbreviations: BTS—Broadtop synclinorium, HRA—Hanging Rock anticline, BMA—Baker Mountain anticline, TRS—Timber Ridge syncline, NMA—North Mountain anticline, ARA—Anderson Ridge anticline, NMF—North Mountain Fault.) Patterns: crosshatch—autochthonous rocks, coarse stipple—Cambro-Ordovician carbonates, fine stipple—Upper Ordovician to Lower Devonian cover.

COVER FOLDING

Fold shape

The dominant mesoscopic and macroscopic structures in the study area are folds (Figs. 4 and 5). Their shapes are of three types — straight limbs and rounded hinges; straight limbs and narrow subangular hinges ('kink' — Boyer 1986, or 'dip domain' — Groshong personal communication); and box or 'liftoff' folds (Namson 1981) (Fig. 5). The second shape is the most common, particularly at smaller scales.

The box or 'liftoff' folds are subisoclinal synclines, which are cored with quartzarenites of the Oriskany Sandstone, and perhaps some basal Devonian shale. Adjacent anticlines are broad, rounder structures of similar amplitude. This geometry could be produced by folding below an upper detachment in the organic-rich Devonian shales. The narrow synclines would be the 'liftoff' folds (Namson 1981), and the anticlines would retain contact with the detachment in the Devonian shales. Such a geometry is able to double the sequence by folding without imbricate faulting (Namson 1981).

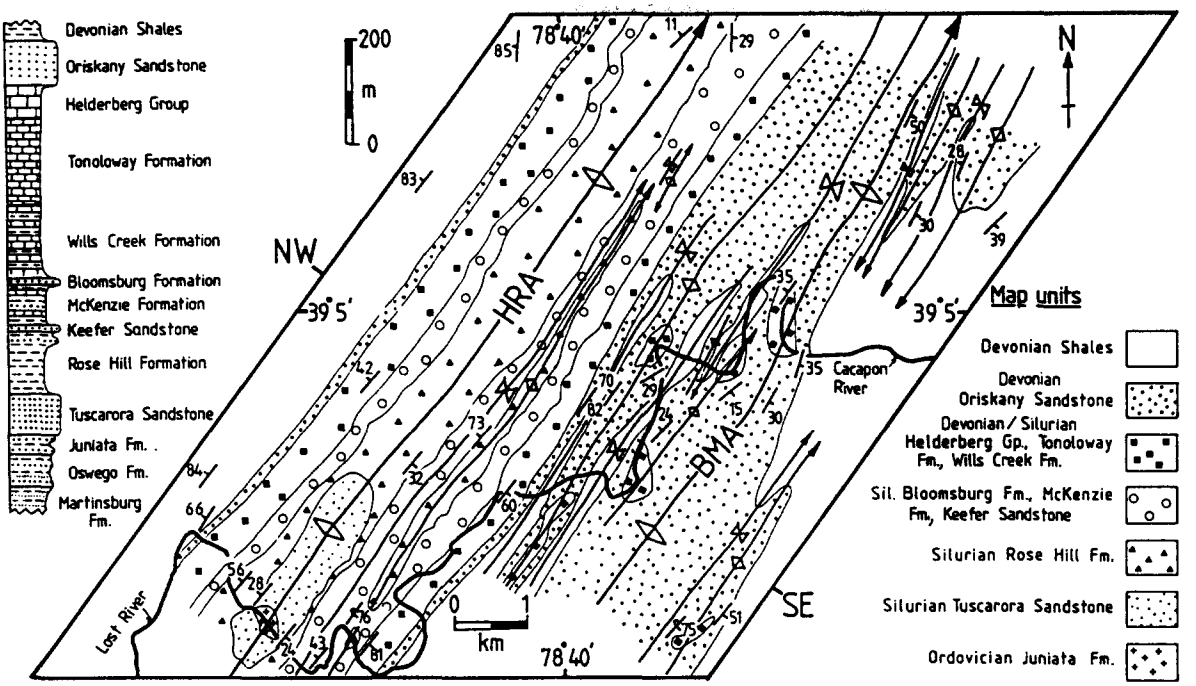

Fig. 4. Stratigraphic column and geological map for study area. NW–SE is section line for Fig. 5. Abbreviations given in Fig. 3.

Detachment also occurs below anticlines that are cored with quartzarenites of the Keefer Sandstone above shales of the Rose Hill Formation. Here, the anticlines are isoclinal with collapsed hinges (Fig. 7a). Therefore, the Ordovician to Devonian cover absorbed large amounts of layer-parallel shortening by very tight folding, rather than by imbricate faulting.

Fold size

The Hanging Rock and Baker Mountain anticlines (Fig. 4) are the only folds large enough to have cores of Cambro-Ordovician carbonates, when projected into the subsurface (Fig. 5). These folds formed passively above the fault-bend and fault-propagation folds of the blind duplex. The many smaller folds, however, range in wavelength from 1.2 km to only centimeters, lack thrust faults and are probably buckle folds.

The smallest folds, with wavelengths of meters to centimeters, are developed in interbedded stiff and soft lithologies, such as limestones and carbonate mudstones, or sandstones and shales. More ductile lithologies, such as wackestones, carbonate mudstones or shales, are consistently uncleaved or weakly cleaved in the small folds (Fig. 6). However, where the same lithologies are not deformed by small folds, they lack interbedded stiffer limestones and sandstones, and they contain cleavage or pencil cleavage. For example, thick shales adjacent to the folds of Fig. 6 are pencil-cleaved (Fig. 7b), unlike the shales in the folds. Therefore, the smaller folds and cleavage are coeval structures, where fold development by buckling of stiffer lithologies precludes cleavage formation.

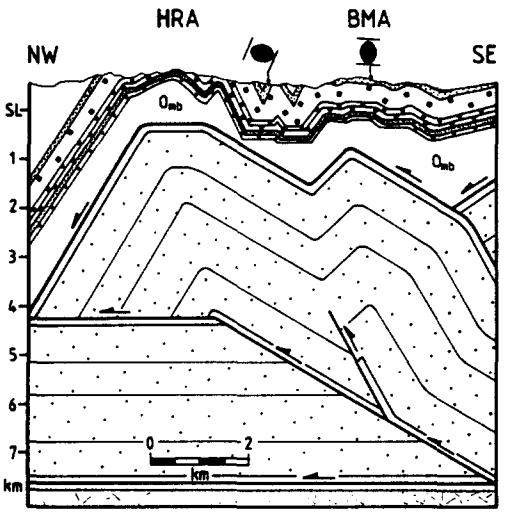

Fig. 5. Cross-section across study area (cover ornament as Fig. 4, Omb–Middle Ordovician Martinsburg Formation, other abbreviations and ornaments as in Fig. 3). Black ellipses for two strain measurements from the Oriskany Sandstone, with short lines for bedding geometry.

COVER FAULTING

Although the cover is extensively folded within the study area, evidence of map-scale faults is absent (Figs. 4 and 5). Also, exposed smaller faults are rare. In fact,

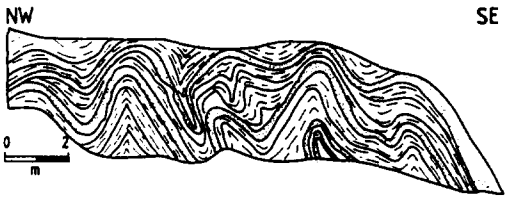

Fig. 6. Disharmonically folded sandstones (stippled beds) with uncleaved shales (dashed beds) in Rose Hill Formation.

the single largest exposed fault displacement is only 15 m on a minor thrust. The area lacks indicators of faults, such as exposed fault traces, juxtaposed stratigraphy or apparently thickened formations. Instead, features such as syncline hinges and normal stratigraphic thicknesses are present in the area, which is consistent with the dominance of folding. It is possible that faults exist in the unexposed parts of the area, but stratigraphy is not juxtaposed and problems of excess space did not occur during section construction. This lack of evidence for faulting is in sharp contrast to the abundance of subsurface thrusting that has been proposed for the Broadtop synclinorium (Figs. 3c & d) to the northwest (Kulander & Dean 1986, Mitra 1986).

COVER CLEAVAGE

Morphology

Cleavage morphology within the cover is dependent on lithology. It ranges from sutured to non-sutured, from anastomosing to smooth planar cleavage (Engelder & Marshak 1985) (Figs. 7c & d and 8a & b) to pencil cleavage (Reks & Gray 1982) (Fig. 7b). The pencil cleavage is restricted to shales of the Silurian Rose Hill Formation and the Devonian shales. Cleavage is typically non-sutured and planar to wavy in siltstones, detrital mudstones and argillaceous carbonate mudstones (Fig. 8b). Wackestones and packstones have non-sutured anastomosing cleavage (Figs. 7d and 8a). Grainstones and non-argillaceous carbonate mudstones have planar sutured cleavage (Fig. 7c).

The cleavage has features that are typical for a solution cleavage (Nickelsen 1972, Geiser 1974, Groshong 1975, 1976, Engelder & Marshak 1985). Cleavage truncates bedding laminations, and clay is preferentially concentrated in the cleavage zones, as opposed to the microlithons.

Geometry

Four observations support the hypothesis that all cleavage was normal to bedding, regardless of lithology, before regional folding. First, cleavage in the siltstones of the Bloomsburg Formation is parallel to *Skolithos* burrows that were initially bedding-perpendicular. Second, mudcracked beds in the Wills Creek Formation, which contain cleavage, are cleaved parallel to mudcracks, which were initially bedding-perpendicular. Third, in beds of the Wills Creek Formation that have deformed mudcracks, the cracks contain abundant crack-parallel microscopic pressure-solution surfaces without additional cleavage. Fourth, many packstones, grainstones and siltstones (Figs. 7c and 8b) contain bedding-perpendicular cleavage regardless of the present bedding attitude.

Cleavage to bedding angles are now significantly larger in grainstones, packstones and siltsones (Figs. 7c & d), than in finer-grained lithologies such as wackestones, carbonate mudstones and shales (Figs. 8a and 7d). Suggested models for the differences in cleavage-to-bedding geometry in different lithologies after folding include: (1) cleavage tracking different *XY* strain planes during folding (Treagus 1982); (2) different mesoscopic deformation events and microscopic deformation mechanisms (Gray 1981); and (3) modification of an initially bedding-perpendicular cleavage during folding (Henderson *et al.* 1986). Given the abundant evidence for cleavage having been initially bedding-perpendicular, the third model is the basis for kinematic analysis of cleavage in the study area.

A combination of graphical techniques (Ramsay 1967, Gray 1981) and strain models (Ramsay 1967, Treagus 1982) can be used to kinematically interpret cleavage geometries (Fig. 10). The graphical techniques are plots for (1) cleavage-to-bedding angle vs bedding dip; (2) fold interlimb angle vs cleavage fan angle; and (3) axial transection vs fold interlimb angle. The strain models are (1) passive rotation of bedding-normal cleavage surfaces during folding by flexural flow; and (2) passive rotation of layer-normal cleavage after folding by late-stage flattening.

For the flexural flow models, curves that are labelled 100F, 50F and 25F are used to represent deformation where 100, 50 and 25%, respectively, of the sequence flexurally flowed (Fig. 9a). For the flattening models, curves that are labelled 0, 10, 20 are used to represent deformation where 0, 10 and 20% horizontal shortening developed, respectively (Fig. 9b).

Cleavage-to-bedding angles for grainstones, packstones, and siltstones almost all exceed 80°. Hence, they are nearly bedding-perpendicular regardless of bedding dip (Fig. 10a). Also, for folds in these lithologies, the sum of the interlimb and cleavage fan angles is about 180° (Fig. 10b). This total of about 180° is consistent with the cleavage-to-bedding angles of about 90° in each of a pair of limbs. Such consistent geometries support the model that the cleavage in these lithologies was initially layer-perpendicular, and was not modified by subsequent folding (Gray 1981). Variations of up to 10° from bedding-normal geometry may have been caused by: (1) cleavage surfaces forming at slightly less than 90° to bedding; (2) late-stage flattening of less than 10% (10 curve, Figs. 10a & b); (3) a small increment of flexural flow during folding. However, the geometric and field data are insufficient to select from these three alternatives.

By contrast, cleavage-to-bedding angles for the wackestones, carbonate mudstones, and detrital mudstones range from 25 to 90° (Figs. 7d, 8a & b and 10a). Also in folds with these lithologies, the total of the interlimb and cleavage fan angles is significantly less than 180° (Fig. 10b). The smaller angles in these lithologies (Figs. 10a & b) plot amongst the curves for flexural flow. For example, detrital mudstones that are less than 50 or 25% of their local sequences in the Bloomsburg, Rose Hill and Juniata Formations plot around the 25F curve in Fig. 10(a). In exposure, the adjacent sandstones and siltstones are uncleaved, and

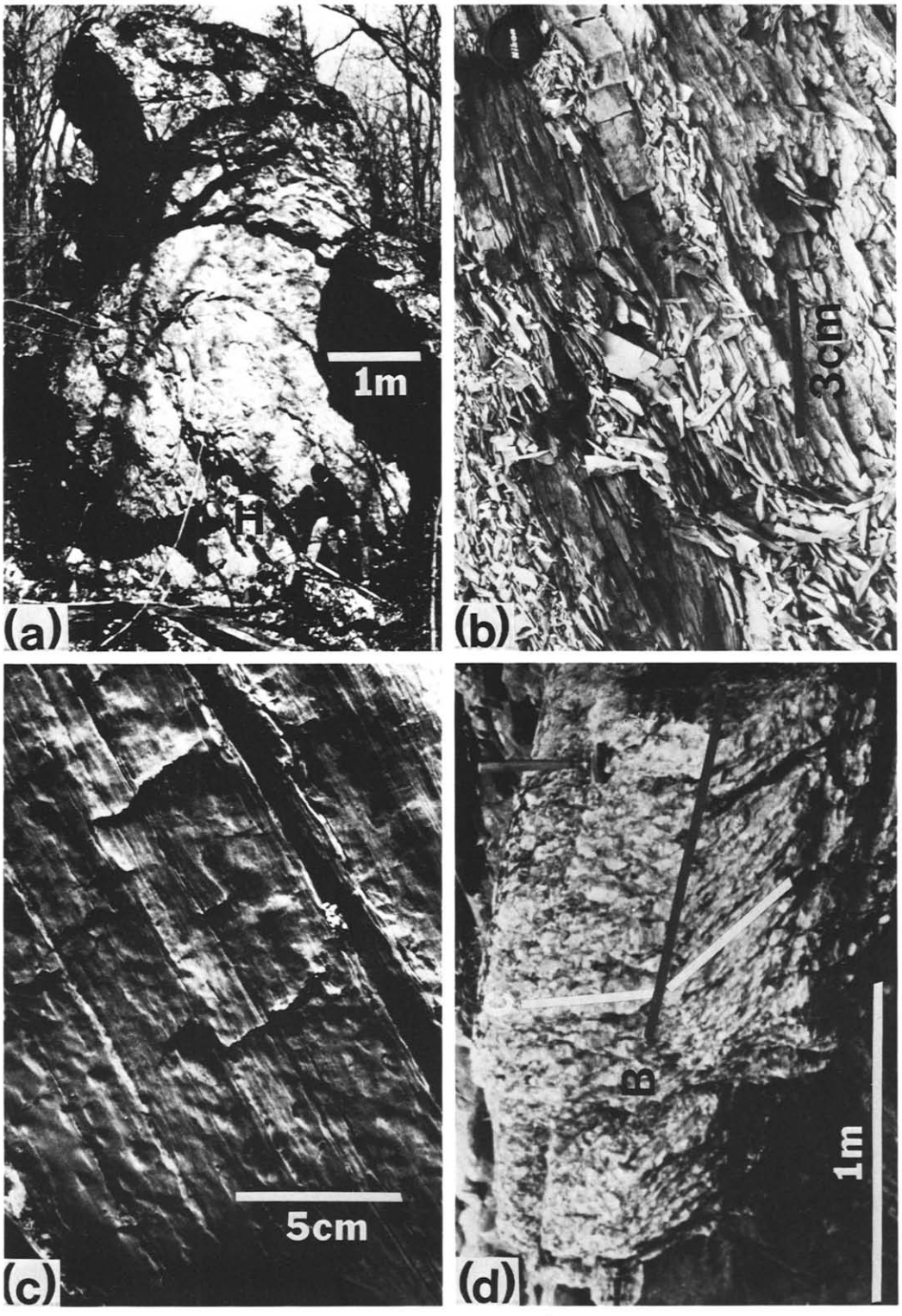

Fig. 7. (a) Isoclinal anticline in the Keefer Sandstone with a collapsed hinge (H) near person for scale. (b) Pencil cleavage in shales of Rose Hill Formation. (c) Bedding-perpendicular stylolitic cleavage in non-argillaceous carbonate mudstone of Tonoloway Formation. (d) Cleavage refraction between a packstone (upper bed) and wackestone (lower bed) in the Helderberg Group (B is bedding, C is cleavage).

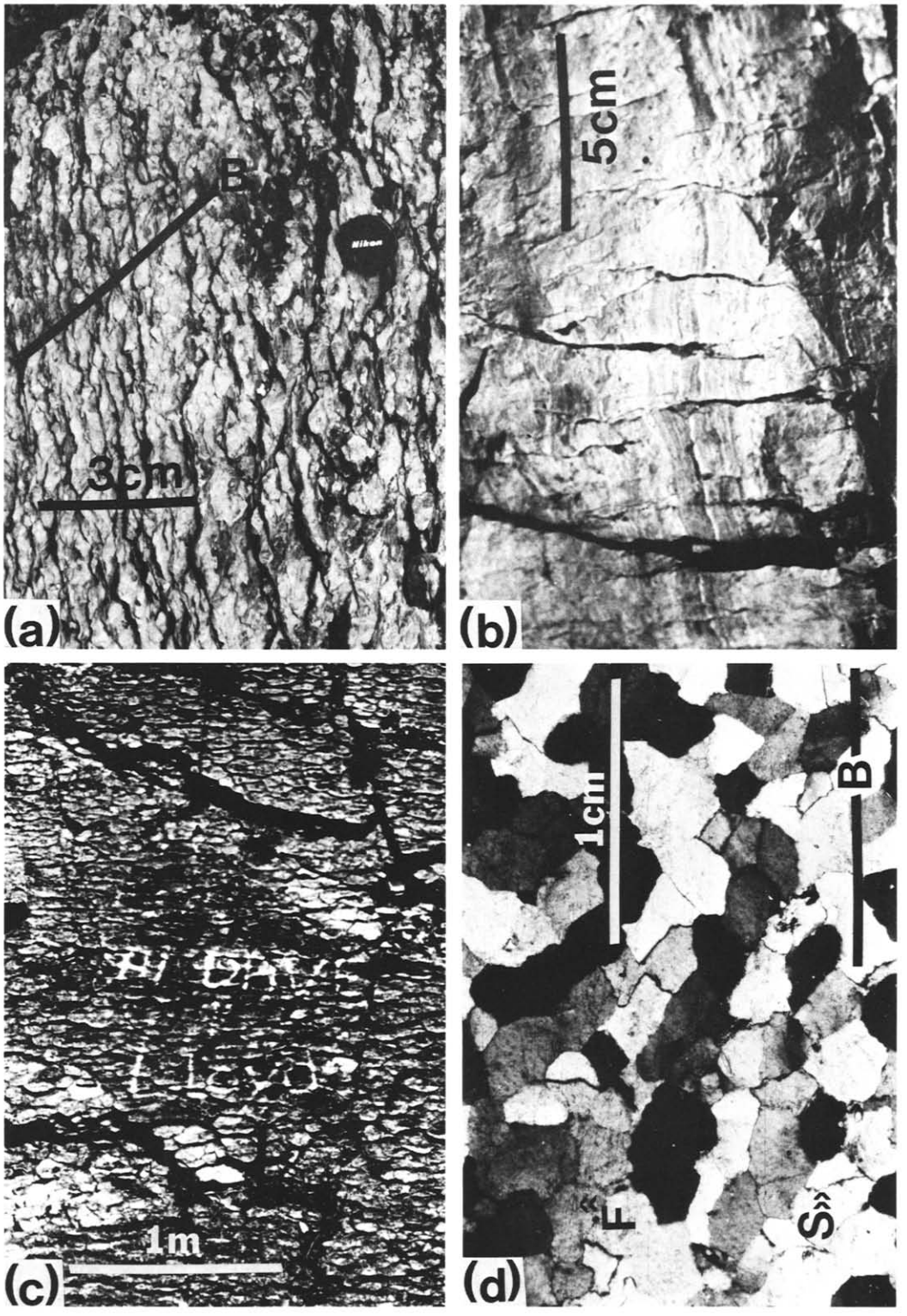

Fig. 8. (a) Anastomosing disjunctive cleavage in wackestone of the Helderberg Group (B is bedding). (b) Pronounced bedding-normal cleavage zones in laminated argillaceous carbonate mudstones of the Tonoloway Formation. (c) Bedding-plane view of deformed mudcracks in laminated carbonate mudstones of the Wills Creek Formation. (d) Photomicrograph of quartzarenite texture in the Oriskany Sandstone (B is bedding trend, S is bedding-subnormal sutured grain contact. F are bedding-parallel fluid inclusion trails).

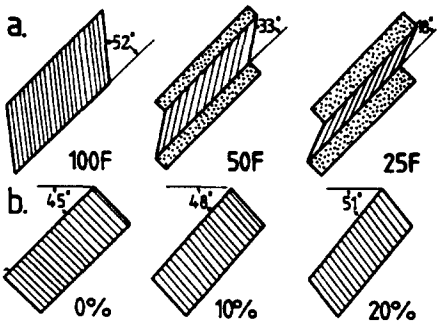

Fig. 9. (a) Example cleavage-to-bedding angles for 45° dip where flexural flow occurs in 100, 50 and 25% of the sequence. (b) Example cleavage-to-bedding angles for a layer with 45° dip that is flattened by 0, 10 and 20%.

some detrital mudstones are bounded by crystal-fiber slickensides. Therefore, cleavage is lithologically restricted to the mudstones and evidence for flexural slip and flow is concentrated in the mudstones and their bedding surfaces. This outcrop geometry and point distribution in the graphs (Figs. 10a & b) indicate that flexural flow was restricted to the mudstones during folding. This interpretation also applies to the wackestones and argillaceous carbonate mudstones, which are represented in Fig. 10(a) adjacent to the 25F and 50F curves.

Many of the wackestones and non-argillaceous carbonate mudstones have cleavage-to-bedding angles over 70° and plot away from the flexural flow curves (Figs. 10a & b). However, these angles of 70–85° are not attributable to 10–20% flattening (10, 20 curves, Figs. 10a & b), because bed thickness in the cleaved units does not change with dip around folds as would be expected for late-stage flattening (Hudleston 1973). Perhaps, these lithologies with these cleavage–bedding angles were deformed by flexural flow during only an increment of folding.

Additional evidence against a late-stage flattening event is provided by data in the graph of fold axial transection vs interlimb angle (Fig. 10c). Gray (1981) determined that axial transection decreases with decreasing interlimb angle if folds were modified by late-stage flattening. In the present study area, transection angles range from 0 to 27° without any correlation to lithology and interlimb angle. Therefore, this data distribution indicates that late stage flattening is absent or very minor. Also, the large variation in transection angle supports the earlier conclusion that the cleavage and folds were initiated at different stages.

Spacing

Cleavage spacing is systematically related to lithology in the study area. Figure 10(d) shows the mean cleavage spacing in lithologies symbolized on the right ends of the dashed lines. In order of decreasing cleavage spacing,

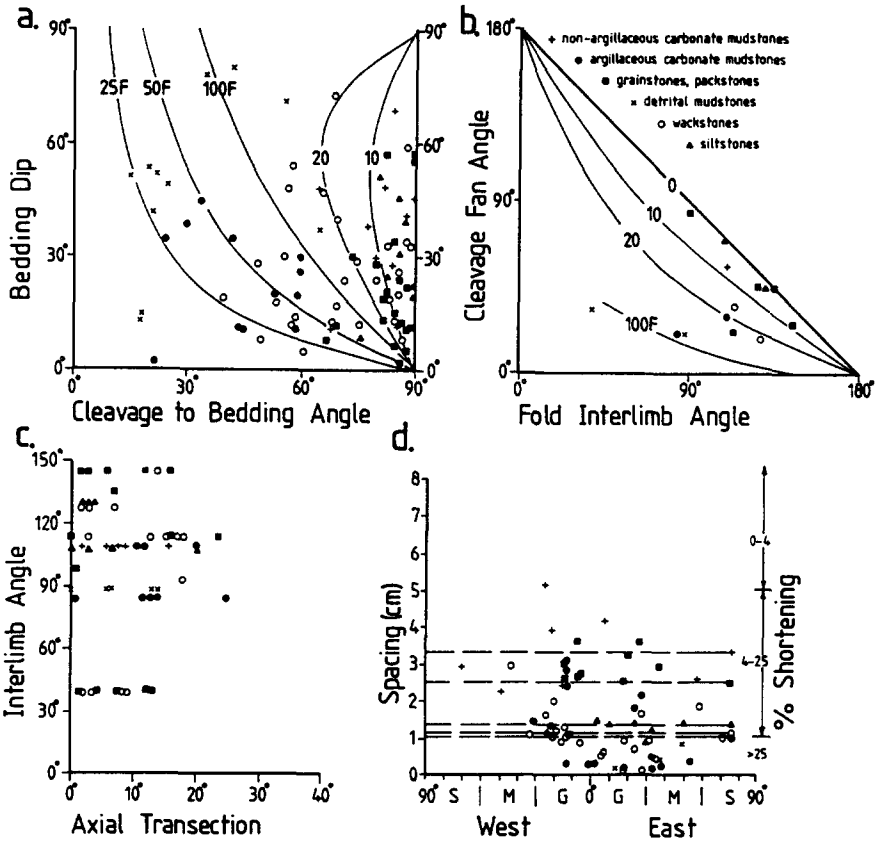

Fig. 10. Cleavage geometry in different lithologies. For (a) and (b), 100F, 50F, 25F are model curves for flexural flow that is compensated for in 100, 50 and 25% of a sequence, respectively. 10 and 20 are model curves for late-stage sub-horizontal flattening of 10 and 20%, respectively. For (c) axial transection is the angle between cleavage and fold axis (Gray 1981). For (d), X axis is bedding dip amount with G—gentle, M—moderate and S—steep. Y axis is distance between centers of cleavage zones. Dashed lines are mean cleavage spacings for lithologies symbolized on right-hand ends of lines.

the means are 3.36 ± 1.02 cm for non-argillaceous carbonate mudstones, 2.48 ± 0.81 cm for packstones and grainstones, 1.43 ± 0.61 cm for siltstones, 1.13 ± 0.13 cm for wackestones and 1.11 ± 1.02 cm for argillaceous carbonate mudstones. Cleavage spacings in detrital mudstones are too small at most exposures to be mesoscopically determined.

Cleavage spacing in packstones, grainstones and siltstones does not systematically vary with changing bed dip. Indeed, the siltstones have almost constant cleavage spacing through the folds. Such constant spacing is consistent with prefolding pervasive cleavage that subsequently was only passively rotated during folding. By contrast, the wackestones decrease spacing with decreasing dip (Fig. 10d). Such an intensification could result from additional cleavage formation in hinges during folding.

The mean cleavage spacings for the limestones were compared with cleavage spacing in pelagic limestones and marls (Alvarez *et al.* 1978) to determine strain magnitudes for the cleavage. All mean spacings indicate strain magnitudes for cleavage formation of 4–25% (Fig. 10d). Also, because the spacings are less than 3.5 cm, the magnitude of the cleavage-forming strain may be closer to 25% than 4%.

Four types of strain measurement support a cleavage-forming strain magnitude of 10–25%. First, one imbricated and uncleaved chert bed that is interbedded with cleaved wackestones has 23% layer-parallel shortening. Second, mudcracks in the Wills Creek Formation show layer-parallel shortening (Fig. 8c). The mudcrack strains were measured using random-line (Sanderson 1977) and Fry (1979) methods. The layer-parallel strains are 18.4 and 16.8%, respectively.

Third, two samples were collected from the Oriskany Sandstone in locations with contrasting dip (Fig. 5, black ellipses). The Fry method was applied to over 100 grain centers in the silica-cemented, well-sorted quartz-arenites of each sample, following the approach of Bowen (1985). The eastern sample in subhorizontal beds has a strain of 13.4% layer-parallel shortening, and the western sample has a 16.4% layer-parallel strain in steeply dipping beds. For both samples, the longer strain axis is layer-normal, irrespective of bed dip. Both samples have grain boundaries that are sutured and subnormal to layering, indicating pressure-solution (S, Fig. 8d). Also, the slightly more-strained western sample has abundant bedding-parallel fluid-inclusion trails (F, Fig. 8d) that cross grain boundaries and cement overgrowths. These microstructures and the strain geometry indicate a layer-parallel shortening event that was then rotated by folding.

Fourth, profile shortening of microfolds in microlithons of pencil-cleaved beds was measured to determine minimum strain from pencil-cleavage formation. The strain magnitude ranges from 9.2 to 20.4% shortening with a mean of 16.0% ± 3.6% (Fig. 11). In all samples, the microfold envelopes are bedding-parallel, regardless of bedding dip. This geometry also indicates an early layer-parallel shortening event with subsequent rotation by folding.

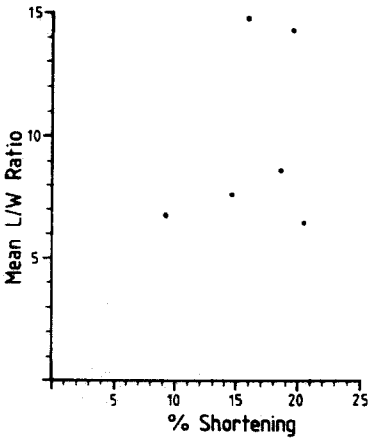

Fig. 11. Strain vs length/width ratios for pencil cleavage.

In summary, the geometric, spatial and strain data for cleavage indicate that cleavage formation predates the development of the large folds. During cleavage formation, about 15% layer-parallel shortening occurred. Interbedded uncleaved lithologies imbricated, developed small folds, pressure-solved along mudcracks or locally on grain boundaries, and fractured at a grain scale. During folding, some cleavage in the finer-grained lithologies was passively rotated by flexural flow. After folding, the area may have been deformed by a very weak flattening event of less than 5%.

DUPLEX GEOMETRY

The macrostructure of the underlying duplex of Cambro-Ordovician carbonates (Fig. 5) was inferred by using these six constraints: (1) the macroscale geometry of the cover from mapping; (2) stratigraphic thicknesses for the carbonates (Perry 1978, Kulander & Dean 1986, Mitra 1986); (3) residual gravity anomalies contrasting the denser Cambro-Ordovician carbonates and less-dense Martinsburg Formation (Ferrill 1987); (4) proprietary seismic reflection data; (5) the assumption of constant thickness for the carbonates; and (6) standard geometries for fault-bend and fault-propagation folds with layer-parallel shear (Suppe 1985, Mitra 1986). The resulting geometry beneath the Hanging Rock anticlinorium consists of a horse with a combination of a fault-bend and fault-propagation folds. This horse is the forelandwardmost of three, forming a major duplex under the cover immediately to the northwest of the North Mountain Fault (Figs. 3 and 12).

COMPARISON OF SHORTENING

The total shortening for the cover in the study area can be represented by equation (1):

$$E_{tc} = E_f + E_i + E_{lps} + E_{lf}, \quad (1)$$

where E_{tc} is the total cover shortening, E_f is the shortening by passive and buckle folding, E_i is the shortening by imbricate faulting, E_{lps} is prefolding layer-parallel shortening that is related to cleavage formation, and E_{lf} is subhorizontal late-stage flattening. The total shortening for the blind duplex can be represented by equation (2):

$$E_{td} = E_i + E_{is}, \quad (2)$$

where E_{td} is the total duplex shortening, E_i is the shortening by imbrication (including fault-bend and fault-propagation folding), and E_{is} is the internal shortening.

For the cover, E_f was measured from the cover folds in Fig. 5; the total shortening is 2.75 km. Faulting is very uncommon in the area; summing all the mesoscopically observed contraction faulting along the section line, $E_i < 0.03$ km. For E_{lps}, the shortening is measured along the presently folded layering, assuming a layer-parallel strain of 15%; hence E_{lps} is equal to 2.16 km. For E_{lf}, shortening is measured along a horizontal datum. Late-stage flattening of the area did not exceed 5%; so, the maximum value for E_{lf} is 0.5 km, with a possible minimum of 0 km for no flattening. Therefore, the total cover shortening in km is:

$$E_{tc} = 2.75 + 0.03 + 2.16 + 0.50 = 5.44 \text{ km}$$

with a minimum of 4.94 km if no flattening occurred.

For the duplex, E_i equals 8.13 km by measurement of profile shortening from Fig. 5. For E_{is}, no direct measurements could be made for the internal strain in the unexposed blind duplex. The nearest data for strain in the carbonates are from about 5 km to the east (Cloos 1971). These data are located in the hangingwall of the North Mountains Fault (Fig. 3) which has been transported more than 50 km (Kulander & Dean 1986, M. Evans personal communication). Using deformed oolites and microstructures, Cloos (1971) demonstrated a 5–10% layer-parallel shortening without volume loss. Because the carbonates under the Hanging Rock anticlinorium have been transported a much shorter distance, an internal strain of only 5% is assumed. Thus, E_{is} is about 0.93 km. Therefore, the total duplex-shortening in km is:

$$E_{td} = 8.13 + 0.93 = 9.06 \text{ km}.$$

The difference between the cover and duplex shortening within the Hanging Rock anticlinorium is 3.62 km. Also, the actual shortening difference is greater because the E_{lps} strain, at least, is older than the formation of the underlying horse. As all cover shortening above the duplex has been considered, additional cover coupling cannot be invoked to account for this shortening difference. Thus, additional forethrusting or backthrusting must have occurred. Since the area does not contain evidence for the backthrusting response such as abundant backthrusts, or hinterland-verging folds and cleavage (Fig. 1b), additional cover forethrusting must have occurred forelandward of the duplex and the study area.

Several investigators (Jacobeen & Kanes 1974, Perry & De Witt 1977, Kulander & Dean 1986, Mitra 1986) have found abundant evidence for forethrusting by cover imbrication in this region.

A variety of geometries (Fig. 3) have been used to depict displacement being transferred forelandwards by forethrusting into the cover. For Kulander & Dean (1986), the total shortening by cover imbrication in the adjacent Broadtop synclinorium (BTS in Fig. 3c) is 13.3 km; and for Mitra (1986) it is 20.5 km. So, sufficient forethrusting deformation exists to accommodate the shortening difference between the cover and underlying blind duplex in the Hanging Rock anticlinorium.

DEFORMATION SEQUENCE

Using the above timing relationships and strain comparison, a deformation sequence can be constructed for cover deformation in the area (Fig. 12). Cover deformation initiated with a layer-parallel shortening event that produced the cleavage, related strains in uncleaved beds, and some of the smaller folds. This deformation was probably in response to forelandwards displacement transfer by forethrusting from the first-formed horses of Cambro-Ordovician carbonates (Figs. 12a & b). Then, the cleavage and related structures were rotated and modified by the formation of macroscale folds. This deformation probably occurred as a coupling response when the cover was passively folded by the emplacement of the blind fault-bend and fault-propagation folds in the Cambro-Ordovician carbonates (Fig. 12c). Additional buckle-folding occurred at this time. Also, displacement from underlying blind folds was transferred forelandwards by forethrusting to produce imbricated cover in the Broadtop synclinorium (Fig. 12c) (Mitra 1986). At this stage, 5% flattening in the anticlinorium may have developed.

An important observation from this sequence is that the deformation in the Hanging Rock anticlinorium can be compared to, but not used to balance, the shortening of the blind horse underneath. Much of the cover deformation is related to the emplacement of earlier hinter-

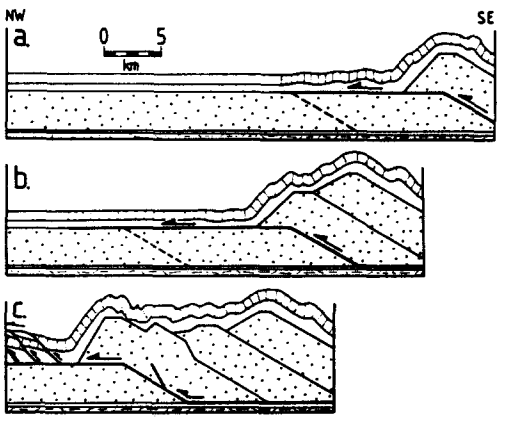

Fig. 12. Schematic deformation sequence through study area for cover and underlying blind duplex. Thin lines in cover show distribution and geometry of cleavage.

landward horses, and is older than the emplacement of the underlying horse (Perry 1978). To actually balance the cover and blind horse, it would be necessary to partition an increment of forethrusting strain from underneath the Broadtop synclinorium to the northwest. Such an approach is beyond the scope of the present study.

One major problem that cannot be answered by the present study is why the style of cover deformation changes from the anticlinorium to the synclinorium. In the Upper Ordovician to Lower Devonian cover of the Hanging Rock anticlinorium, imbricate faulting is uncommon. Whereas, for the same rocks in the subsurface of the Broadtop synclinorium, imbricate faulting is the dominant structure (Jacobeen & Kanes 1974, Perry & De Witt 1977, Kulander & Dean 1986, Mitra 1986).

CONCLUSIONS

(1) The Upper Ordovician to Lower Devonian cover has shortened 5.44 km in the Hanging Rock anticlinorium above blind fault-bend and fault-propagation folds that shortened the Cambro-Ordovician carbonates by 9.06 km.

(2) Cover layer-parallel shortening predated the underlying blind folds as a forethrusting response to the emplacement of horses in the hinterland. The cover responded by coupling, with passive folding and possibly minor flattening, during the emplacement of the blind folds in the Cambro-Ordovician carbonates. Additionally, the cover forelandwards of the study area was deformed by forethrusting to accommodate the blind folds under the study area. By contrast, this forethrusting involved imbricate thrusting rather than the cleavage and fold formation of the earlier forethrusting. Also, the later forethrusting may account for the shortening difference between the blind duplex and cover.

Acknowledgements—David Ferrill acknowledges support of an Appalachian Basin Industrial Associates grant. The authors thank Steven Gerritsen for the quartzarenite strain analyses, Nicholas Woodward for suggesting a fault-propagation fold and Peter Geiser for his preprint.

REFERENCES

Alvarez, W., Engelder, T. & Geiser, P. A. 1978. Classification of solution cleavage in pelagic sediments. *Geology* **6**, 263–266.

Banks, C. J. & Warburton, J. 1986. 'Passive-roof' duplex geometry in the frontal structures of Kirthar and Sulaiman mountain belts, Pakistan. *J. Struct. Geol.* **8**, 229–238.

Bowen, J. H. 1985. Regional finite strain analysis of basal Devonian orthoquartzites: Valley and Ridge Province, Pennsylvania. *Geol. Soc. Am. Abs. W. Prog.* **17**, 6.

Boyer, S. 1986. Styles of folding within thrust sheets: examples from the Appalachians and Rocky Mountains of the U.S.A. and Canada. *J. Struct. Geol.* **8**, 325–339.

Cloos, E. 1971. *Microtectonics Along the Western Edge of the Blue Ridge, Maryland and Virginia. Studies in Geology* No. 20. Johns Hopkins Press, Baltimore.

De Poar, D. G. & Anastasio, D. J. 1987. The Spanish External Sierra: a case history in the advance and retreat of mountains. *Nat. Geogr. Res.* **3**, 199–209.

Dunne, W. M. & Ferrill, D. A. 1988. Blind thrust systems. *Geology* **16**, 33–36.

Engelder, T. & Marshak, S. 1985. Disjunctive cleavage formed at shallow depths in sedimentary rocks. *J. Struct. Geol.* **7**, 327–343.

Ferrill, D. A. 1987. Analysis of shortening across Cacapon Mountain anticlinorium in the central Appalachians of West Virginia. Unpublished M.Sc. thesis, West Virginia University, Morgantown, West Virginia, U.S.A.

Ferrill, D. A. & Dunne, W. M. 1986. Analysis of differential shortening across the Hanging Rock anticline, West Virginia. *Geol. Soc. Am. Abs. W. Prog.* **18**, 220.

Fry, N. 1979. Random point distributions and strain measurement in rocks. *Tectonophysics* **60**, 89–105.

Geiser, P. A. 1974. Cleavage in some sedimentary rocks of the central Valley and Ridge Province, Maryland. *Bull. geol. Soc. Am.* **85**, 1399–1412.

Geiser, P. A. 1988. The role of kinematics in the construction and analysis of geological cross-sections in deformed terrains. In: *Geometries and Mechanisms of Thrusting, with Special Reference to the Appalachians* (edited by Mitra, G. & Wojtal, S.). *Spec. Pap. geol. Soc. Am.* **222**, 47–76.

Geiser, P. A. & Engelder, T. 1983. The distribution of layer parallel shortening fabrics in the Appalachian foreland of New York and Pennsylvania: evidence for two non-coaxial phases of the Alleghenian orogeny. In: *Contributions to the Tectonics and Geophysics of Mountain Chains* (edited by Hatcher, R. D., Williams, H. & Zietz, I.). *Mem. geol. Soc. Am.* **158**, 161–175.

Gray, D. R. 1981. Cleavage-fold relationships and their implications for transected folds: an example from central Virginia. *J. Struct. Geol.* **3**, 265–277.

Groshong, R. H. Jr. 1975. "Slip" cleavage caused by pressure solution in a buckle fold. *Geology* **3**, 411–413.

Groshong, R. H., Jr. 1976. Strain and pressure solution in the Martinsburg Slate, Delaware Water Gap, New Jersey. *Am. J. Sci.* **276**, 1131–1146.

Henderson, J. R., Wright, T. O. & Henderson, M. N. 1986. A history of cleavage and folding: an example from the Goldenville Formation, Nova Scotia. *Bull. geol. Soc. Am.* **97**, 1354–1366.

Herman, G. C. 1984. A structural analysis of a portion of the Valley and Ridge Province of Pennsylvania. Unpublished M.Sc. thesis, University of Connecticut, Storrs, Connecticut, U.S.A.

Hudleston, P. J. 1973. Fold morphology and some geometrical implications of theories of fold development. *Tectonophysics* **16**, 1–46.

Jacobeen, F., Jr. & Kanes, W. H. 1974. Structure of Broadtop synclinorium and its implications for Appalachian structural style. *Bull. Am. Ass. Petrol. Geol.* **58**, 362–375.

Jones, P. B. 1982. Oil and gas beneath east-dipping underthrust faults in the Alberta foothills. In: *Geological Studies of the Cordilleran Thrust Belt* (edited by Powers, R. B.). *Rocky Mountain Ass. Petrol. Geol.*, 61–74.

Kulander, B. R. & Dean, S. L. 1986. Structure and tectonics of central and southern Appalachian Valley and Ridge and Plateau Provinces, West Virginia and Virginia. *Bull. Am. Ass. Petrol. Geol.* **70**, 1674–1684.

Marshak, S. & Engelder, T. 1985. Development of cleavage in limestones of a fold-thrust belt in eastern New York. *J. Struct. Geol.* **7**, 345–359.

McMechan, M. E. 1985. Low-taper triangle-zone geometry: an interpretation for the Rocky Mountain foothills, Pine Pass–Peace River area, British Columbia. *Bull. Can. Petrol. Geol.* **33**, 31–38.

Mitra, S. 1986. Duplex structures and imbricate thrust systems: geometry, structural position, and hydrocarbon potential. *Bull. Am. Ass. Petrol. Geol.* **70**, 1087–1111.

Morley, C. K. 1986a. A classification of thrust fronts. *Bull. Am. Ass. Petrol. Geol.* **70**, 12–25.

Morley, C. K. 1986b. Vertical strain variations in the Osen–Røa thrust sheet, northwestern Oslo Fjord, Norway. *J. Struct. Geol.* **8**, 621–632.

Namson, J. 1981. Structure of the western foothills belt, Miaoli-Hsinchu area, Taiwan: (I) southern part. *Petrol. Geol. Taiwan* **18**, 31–51.

Nickelsen, R. P. 1972. Attributes of rock cleavage in some mudstones and limestones of the Valley and Ridge Province, Pennsylvania. *Proc. Pennsylvania Acad. Sci.* **46**, 107–112.

Perry, W. J., Jr. 1978. Sequential deformation in the central Appalachians. *Am. J. Sci.* **278**, 518–542.

Perry, W. J., Jr. 1979. The Wills Mountain anticline: a study in

complex folding and faulting in eastern West Virginia. *W. V. Geol. Econ. Surv. Publs*, RI-32.

Perry, W. J., Jr. & De Witt, W., Jr. 1977. A field guide to thin-skinned tectonics in the Central Appalachians. *Am. Ass. Petrol. Geol. Annual Convention Field Trip* 4.

Ramsay, J. G. 1967. *Folding and Fracturing of Rocks*. McGraw-Hill, New York.

Reks, I. J. & Gray, D. R. 1982. Pencil structure and strain in weakly deformed mudstone and siltstone. *J. Struct. Geol.* **4**, 161–175.

Sanderson, D. J. 1977. The analysis of finite strain, using lines with an initial random orientation. *Tectonophysics* **88**, 201–233.

Suppe, J. 1983. Geometry and kinematics of fault-bend folding. *Am. J. Sci.* **283**, 684–721.

Suppe, J. 1985. *Principles of Structural Geology*. Prentice-Hall, Englewood Cliffs, New Jersey.

Treagus, S. H. 1982. A new isogon-cleavage classification and its application to natural and model fold studies. *Geol. J.* **17**, 49–64.